

Supporting Information

Sterky et al. 10.1073/pnas.1103295108

SI Materials and Methods

Breeding and Handling of Mice. Mice carrying a loxP-flanked *Tfam* allele (1) were crossed for two consecutive generations with mice carrying the *Gt(ROSA26)Sor^{Stop-mito-YFP}* allele to generate mice with the genotype *Tfam^{loxP/+};Gt(ROSA26)Sor^{Stop-mito-YFP/Stop-mito-YFP}*. These mice were mated to mice with the genotype *DAT^{cre/cre};Tfam^{loxP/+}* to generate MitoPark mice (*DAT^{cre/+};Tfam^{loxP/loxP};Gt(ROSA26)Sor^{Stop-mito-YFP/+}*) and controls (*DAT^{cre/+};Tfam^{+/+};Gt(ROSA26)Sor^{Stop-mito-YFP/+}*) with labeled mitochondria. For injection experiments, mice with the genotype (*DAT^{cre/+};Tfam^{loxP/+};Gt(ROSA26)Sor^{Stop-mito-YFP/+}*) were mated to *Tfam^{loxP/loxP}* mice and also used as controls.

Mice with disruption of exon 3 of Parkin (2) were bred to mice with the genotype *Tfam^{loxP/loxP}*. The resulting double-heterozygous mice were mated in turn to mice with the genotype *DAT^{cre/+};Tfam^{loxP/loxP};Gt(ROSA26)Sor^{Stop-mito-YFP/+}*. Selected Parkin heterozygous offspring from this mating were interbred in turn to generate MitoPark mice with labeled mitochondria either with Parkin (*Parkin^{+/+};DAT^{cre/+};Tfam^{loxP/loxP};Gt(ROSA26)Sor^{Stop-mito-YFP/+}*) or without Parkin (*Parkin^{-/-};DAT^{cre/+};Tfam^{loxP/loxP};Gt(ROSA26)Sor^{Stop-mito-YFP/+}*). Offspring without the YFP reporter allele were used for cell counts.

To generate mice with ubiquitous expression of mito-YFP, mice carrying the *Gt(ROSA26)Sor^{Stop-mito-YFP}* allele were crossed to mice expressing *cre* under control of the β -actin (*Actb*) promoter (1). Double-heterozygous offspring from this mating were backcrossed to generate *Gt(ROSA26)Sor^{mito-YFP/+}* (mito-YFP⁺) and wild-type littermates used for biochemical measurements.

All animal experiments were approved by animal welfare committees (Stockholm North and South, respectively) and performed in compliance with Swedish law.

Southern Blot and Genotyping. Genomic DNA from ES cell lysates and mouse-tail cuts were isolated using the DNeasy kit (Qiagen) and digested overnight in restriction enzyme mix. Fragments were separated on a 0.6% agarose gel and transferred to a nylon membrane (Amersham Bioscience). Probes were labeled with [³²P]-dCTP by random priming using the Prime-IT II kit (Stratagene). Probe p1 was generated by PCR from genomic DNA (primers 5'-gaattcatgctactgactgg and 5'-tgaccaaggctcttggcc).

Genotyping of the ROSA26 locus was performed using primers ROSA26-R1, ROSA26-R2, and ROSA26-R3 as previously described (3). The recombined allele gives rise to an ~380-bp band using primers ROSA26-R1 and ROSA26-R4 (5'-attagacagcatgtaccaagc).

Biochemical Measurements. Respiratory chain enzyme activities and mitochondrial ATP production rates were measured in heart mitochondria from 20-wk-old mito-YFP⁺ mice and littermate controls as previously described (4, 5). Citrate synthase (CS) and activity were determined in heart tissue samples and used as a mitochondrial marker.

Tissue Processing and Immunohistochemistry. Mice were deeply anesthetized with pentobarbital and subjected to transcatheter perfusion with heparinized Ca²⁺-free Tyrode's solution followed by 4% paraformaldehyde with 0.4% picric acid in 0.16 M phos-

phate buffer. Brains were dissected, postfixed, and thereafter equilibrated with 10% sucrose in phosphate buffer. Brains were frozen on CO₂ ice and cryosectioned to obtain 14- or 20- μ m sections. Sections were rehydrated and mounted (Vectashield; Vector Laboratories). For immunohistochemistry, tyrosine hydroxylase (TH) (1:500; Sigma), TOM20 (1:2,000; Santa Cruz), superoxide dismutase 2 (1:200; Upstate), and Cy3-conjugated secondary antibodies (1:400; Jackson ImmunoResearch) were used.

Stereology. Serial 20- μ m sections of midbrains from 31.5 \pm 1-wk-old littermate MitoPark mice with or without Parkin were stained with an antibody against TH (1:500; Pel-Freez) and a peroxidase-based chromogen (Vector SG; Vector Laboratories). Nuclei of TH-immunoreactive cells in substantia nigra pars compacta (SNc) on both sides were counted with blinded genotype using stereology (Stereologer v. 2001; Stereology Resource Center).

Stereotactic Injections. Mice were anesthetized with isoflurane and buprenorphine (0.075 mg/kg s.c.) and put in a stereotactic frame (Stoelting). After a midline skin incision was made, a burr hole was made over the midbrain or striatum. Viral constructs (typically 1 \times 10⁹ viral genomes in 2 μ L PBS) were injected into the substantia nigra (2.9 mm caudal to bregma, 1.3 mm lateral to the midline, and 4.2 mm ventral to dura mater) using a 10- μ L Hamilton syringe with a custom-made 33-G needle (45° type 4 tip) connected to a microsyringe pump controller (World Precision Instruments). The volume was injected over 5–6 min, and the needle was left in situ for another 4 min before retraction. The scalp was closed using a 6–0 Ethicon suture.

Retrograde tracing using fluorogold was performed essentially as described (6). Fluoro-Gold (20 mg/mL in 0.2 μ L saline) (Fluorochrome, LLC) was delivered to striatum (0.7 mm anterior to bregma, 1.8 mm lateral to the midline, and 2.6 mm ventral to dura mater) using a similar syringe, needle, and injection regime as described above.

Western Blot. Total protein extracts from brains of Parkin-knockout and wild-type mice were separated by SDS/PAGE and transferred to a PVDF membrane (Millipore). Antibodies against Parkin (PRK8; 1:2,000; Sigma) and actin (1:5,000; Abcam) were used for detection and visualized by chemiluminescence (ECL).

Cell Culture. Wild-type HeLa cells were grown in DMEM with 10% FBS and antibiotics. Cells were plated on coverslips and transiently transfected with the adeno-associated virus (AAV)-Cherry-Parkin expression vector using Fugene HD (Roche). Forty-eight hours later, cells were exposed to 10 μ M carbonyl cyanide *m*-chlorophenylhydrazone (CCCP) or DMSO (0.1%) for 1 h. Cells were fixed with 4% paraformaldehyde and stained for TOM20 with an Alexa 488-conjugated secondary antibody.

Statistical Analysis. Statistical significance was assessed by two-tailed student *t* tests or one-way ANOVA with Bonferroni post hoc correction. Unilateral injections were treated as independent experiments.

1. Larsson NG, et al. (1998) Mitochondrial transcription factor A is necessary for mtDNA maintenance and embryogenesis in mice. *Nat Genet* 18:231–236.
2. Itier JM, et al. (2003) Parkin gene inactivation alters behaviour and dopamine neurotransmission in the mouse. *Hum Mol Genet* 12:2277–2291.

3. Soriano P (1999) Generalized lacZ expression with the ROSA26 Cre reporter strain. *Nat Genet* 21:70–71.
4. Wibom R, Hagenfeldt L, von Döbeln U (2002) Measurement of ATP production and respiratory chain enzyme activities in mitochondria isolated from small muscle biopsy samples. *Anal Biochem* 311:139–151.

5. Wredenberg A, et al. (2002) Increased mitochondrial mass in mitochondrial myopathy mice. *Proc Natl Acad Sci USA* 99:15066–15071.

6. Sieber BA, et al. (2004) Disruption of EphA/ephrin-a signaling in the nigrostriatal system reduces dopaminergic innervation and dissociates behavioral responses to amphetamine and cocaine. *Mol Cell Neurosci* 26:418–428.

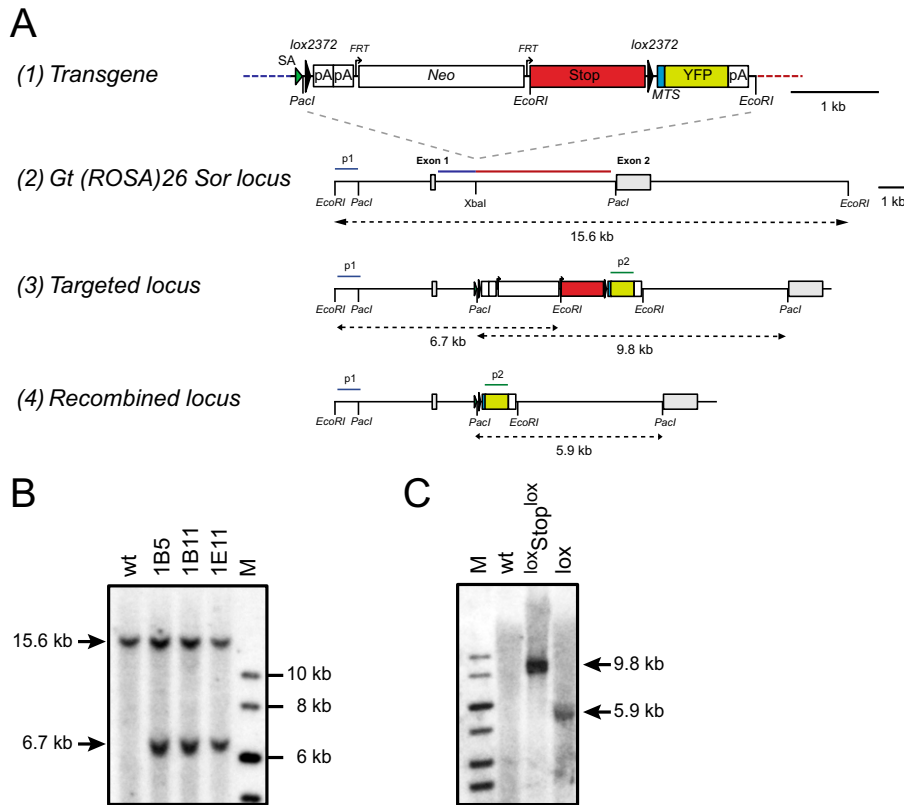


Fig. S1. Design of lox-Stop-lox-mito-YFP and targeting to the ROSA26 locus. (A) Insertion of the lox-Stop-lox-mito-YFP transgene (1) in the Gt(ROSA)26Sor locus (2). YFP fused to a mitochondrial targeting sequence (MTS) is placed downstream of a stop cassette, which contains tandem poly-adenylation signals (pA), a Westphal stop cassette (Stop), and a neomycin resistance gene (Neo), flanked by heterologous loxP-sites (lox2372). The construct is inserted downstream of exon 1 in the ROSA26 locus by homologous recombination (3). The short and long homology arms are shown in blue and red, respectively. When the stop cassette is removed by cre-mediated excision (4), fusion between the noncoding ROSA26 exon 1 and an introduced splice acceptor (SA) allows transgene expression by the endogenous ROSA26 promoter. FRT, Flippase recognition target. (B) Identification of targeted ES clones by restriction digest of genomic DNA with EcoRI and hybridization with an external probe (p1). Insertion of a novel EcoRI site in the transgene gives rise to a 6.7-kb fragment in targeted clones. (C) Germline transmission and removal of the stop cassette. DNA isolated from tail biopsies of wild-type, targeted ROSA26^{+/SmY} mice (lox-Stop-lox) and in ubiquitously recombined ROSA26^{+/SmY};β-actin-cre mice (lox) were subjected to genomic digest with Pacl and hybridization with an internal probe (p2).

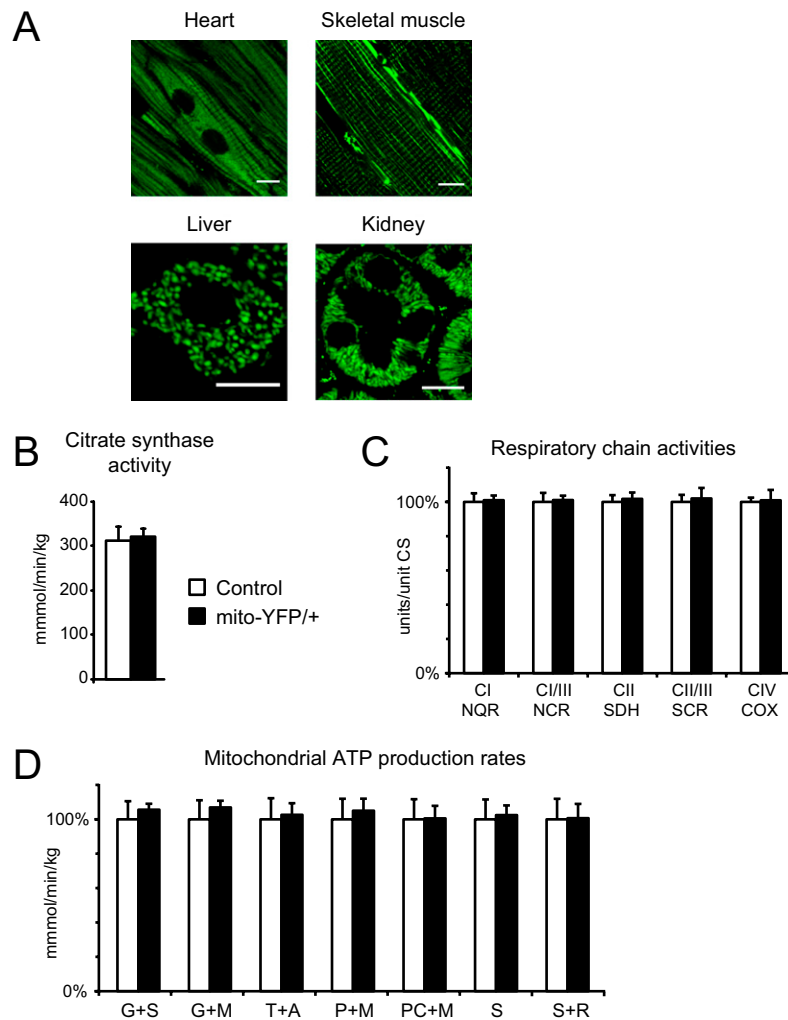


Fig. S2. Ubiquitous expression of mito-YFP does not affect mitochondrial respiration. (A) YFP-labeled mitochondria in heart muscle, skeletal muscle fibers, a liver hepatocyte, and kidney tubules in mice with ubiquitous mito-YFP expression (genotype ROSA26^{+/SmY};β-actin-cre). (Scale bars: 10 μm.) (B–D) Biochemical measurements of mitochondrial enzyme activities in heart tissue from control mice (open bars) and mito-YFP/+ mice (black bars) at age 20 wk. Data are shown as mean ± SEM ($n = 5$). (B) CS activity in heart tissue. (C) Respiratory-chain enzyme activities in mitochondrial preparations from hearts. Complex I (NADH coenzyme Q reductase, NQR), complexes I plus III (NADH cytochrome c reductase, NCR), complex II (succinate dehydrogenase, SDH), complexes II plus III (succinate:cytochrome c reductase, SCR), and complex IV (cytochrome c oxidase, COX) were measured and normalized to CS activity in the mitochondrial suspension. The relative enzyme activities presented as 100% in the figure correspond to the following absolute ratios of enzyme activities per unit of CS activity: NQR, 0.76; NCR, 0.29; SDH, 0.33; SCR, 0.49; COX, 2.44. (D) ATP production rate in intact, isolated mitochondria in the presence of substrates glutamate plus succinate (G+S), glutamate plus malate (G+M), *N,N,N,N*-Tetramethyl-*p*-Phenylenediamine (TMPD) plus ascorbate (T+A), pyruvate plus malate (P+M), palmitoyl-L-carnitine plus malate (PC+M), succinate (S), and succinate plus rotenone (S+R). The relative enzyme activities presented as 100% in the figure correspond to the following absolute mitochondrial ATP production rates per kg of heart muscle: G+S, 335; G+M, 262; T+A, 280; P+M, 202; PC+M, 169; S, 42; and S+R, 60.

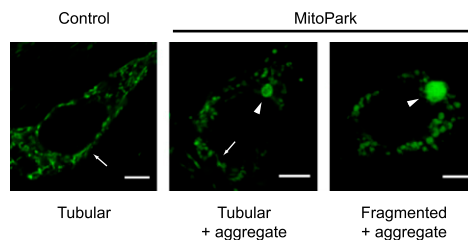


Fig. S3. Examples of mitochondrial morphologies. Respiratory chain-deficient dopamine (DA) neurons were classified based on the presence of at least one tubular mitochondrion (arrows) and/or large mitochondrial aggregate (defined as spherical mitochondria with a diameter >1 μm; arrowheads) visible in the soma. The proportion of MitoPark cells with aggregates may be underestimated because cells may contain aggregates further away from the nucleus. (Scale bars: 5 μm.)

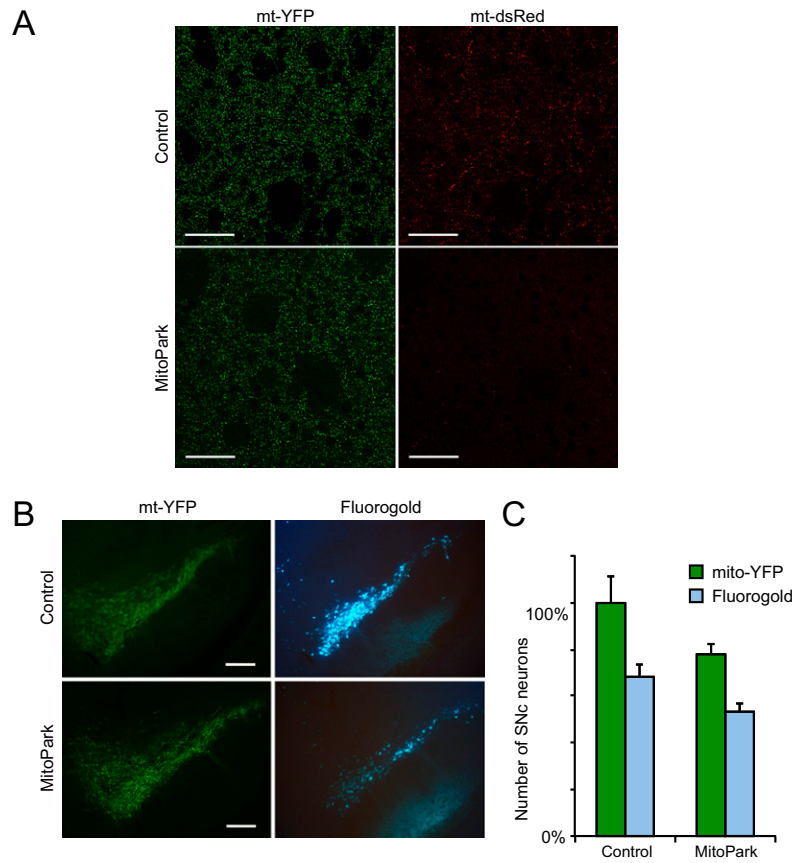
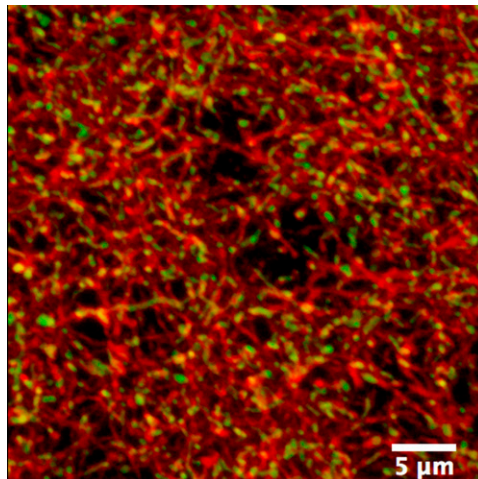


Fig. S6. Axonal transport of mitochondria is impaired. (A) Low-magnification image of striatum with mitochondria that contain YFP and dsRed. (Scale bars: 50 μm .) (B) Mito-YFP- and fluorogold-labeled neurons in SNc 48 h after fluorogold injections in striatum. (Scale bars: 200 μm .) (C) Quantification of mito-YFP- and fluorogold-labeled neurons in SNc. Error bars indicate SEM. ($n = 4$).



Movie S1. Mitochondria in distal axons. 3D rotational volume of YFP-labeled mitochondria (green) in striatal DA fibers (counterstained for TH; red). The stack was noise-reduced by applying a median filter. (Scale bar: 5 μm .)

[Movie S1](#)